CrystEngComm

Snowflake Porous Multi-Metal Oxide Nanocatalysts from Metallocene@Metal Organic Framework Precursors

Journal:	*CrystEngComm*
Manuscript ID	CE-COM-11-2020-001666.R1
Article Type:	Communication
Date Submitted by the Author:	14-Dec-2020
Complete List of Authors:	Luz, Ignacio; RTI International, Parvathikar, Sameer; RTI International Carpenter, Michael; RTI International Grillo, Brittany; RTI International Carpenter, John; RTI International Lail, Marty; RTI International

COMMUNICATION

Snowflake Porous Multi-Metal Oxide Nanocatalysts from Metallocene@Metal Organic Framework Precursors

Received 00th January 20xx,
Accepted 00th January 20xx

DOI: 10.1039/x0xx00000x

Ignacio Luz, Sameer Parvathikar, Michael Carpenter, Brittany Grillo, John Carpenter and Marty Lail*

We report a general approach to prepare 'snowflake' porous metal oxide nanostructured catalysts using tailored precursors consisting on metallocene embedded within MOFs via thermal treatment under air. The resulting well-dispersed multi-metallic nanocatalysts show improved activity for ammonia synthesis at low temperature.

As an alternative to traditional synthetic routes, metal organic frameworks (MOFs) have emerged as versatile precursors for the preparation of porous functional materials based on metal, metal oxides, carbonaceous species, and combinations thereof, exhibiting unprecedented nanostructures. These have been applied as advanced heterogeneous catalysts and electrocatalysts for emerging technologies, ranging from batteries or fuel cells to low-temperature ammonia synthesis[1, 2]. The advantage of using MOFs as precursors to obtain nanostructured catalysts is mainly due to their unique and tailored features, such as well-defined metal sites spaced by organic struts displayed along a crystalline structure with permanent porosity, which can be transferred to the derived materials. Specifically, MOFs can act as both template and precursor, upon applying the proper treatment conditions at high temperature, such as controlled pyrolysis under nitrogen, calcination under air, or reduction under hydrogen[3].

Volatile metallocenes have been demonstrated to be excellent metal precursors due to their ability to infiltrate MOF cavities in the gas phase (metallocene@MOF) for the subsequent formation of a variety of hybrid materials and composites, i.e. metal and metal oxide nanocrystals confined within MOFs, upon photoreduction with UV or chemical reduction with H_2[4, 5]. To do so, MOF pore apertures must be larger than metallocene molecular dimensions to allow the gas-phase infiltration, enabling high loadings of these organometallics within MOF cavities.

RTI International, 3040 E. Cornwallis Rd, RTP, North Carolina, United States.
† Footnotes relating to the title and/or authors should appear here.
Electronic Supplementary Information (ESI) available: [details of any supplementary information available should be included here]. See DOI: 10.1039/x0xx00000x

Here, we take the advantage of the efficient incorporation of metallocenes via gas-phase infiltration within MOFs to prepare porous nanocatalysts. These display well-dispersed, muti-metallic oxide species upon subsequent thermal treatment at specific calcination conditions. This technique can be extended to any MOF exhibiting small pore size windows (< 1 nm), which provides strong molecular confinement to retain the metallocene up to its temperature of oxidation under air within the MOF pores (200-300 ˚C). This confinement effect is often indicated by metallocene release temperatures from the MOF pores being higher than infiltration temperatures (i.e. metallocene boiling point), as demonstrated for ferrocene within UiO-66 in contrast to UiO-67[5]. From the point of view of catalyst design, suitable MOF structures (i.e. MIL-53, MOF-74, MIL-47, HKUST-1, ZIF-n) can incorporate several metals at the nodes (i.e. Fe, Cr, Al, Ga, In or Sc for MIL-53; or Co, Ni, Fe, Mn, Cu or Mn for MOF-74). In addition, there are a large collection of commercially available volatile metallocenes, typically used for chemical vapor deposition, of the type MCp_2 (M= Fe, Ni, Co, Ru, Cr, V or Rh; Cp = cyclopentadienyl), or MCp_2X_2 (M= Ti, Mo, Nb or Zr; X=Cl), that can be selected, which offers a large variety of possible metallocene@MOF combinations (see Scheme S1). Furthermore, we have also demonstrated the controlled and sequential addition of different metallocenes within the same MOF cavities to prepare multimetallic catalysts.

To illustrate our approach, we have selected ferrocene@(Al)MIL-53 as the metallocene@MOF precursor to demonstrate the ability to form well-dispersed iron oxide sub-nanometric species within a snowflake-shaped, porous aluminum oxide support upon calcination under air at moderate temperatures (i.e. 300-500 ˚C). The resulting material has been evaluated as advanced iron catalysts for ammonia synthesis at low-temperature[1].

According to TGA analysis under nitrogen (see Figure S1), up to 35.6 wt.% of ferrocene can be infiltrated within (Al)MIL-53 at 120 ˚C, which produces $(FeCp_2)_{0.62}$@(Al)MIL-53. As indicated earlier, higher temperatures (200-300 ˚C) are required for its release, due to its reduced diffusion within the MOF channels.

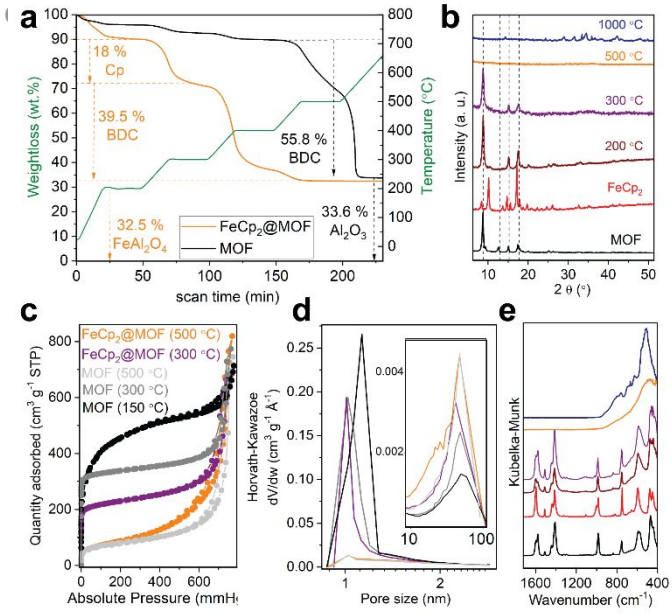

Figure 1. Characterization data for $FeCp_2$@MOF treatment under air compared to bare MOF: a) TGA, b) XRD patterns, c) N_2 sorption isotherms, d) pore distribution, and e) FTIR spectra. Surface area for non-treated $FeCp_2$@MOF is 33 m^2/g according to literature[6].

Meilikhov et. al.[6] reported that the thermal stability of (Al)MIL-53 framework is preserved upon ferrocene release under inert conditions (up to 500 ˚C). In contrast, intrapore oxidation of most of the infiltrated $FeCp_2$ (only 10 wt.% of weakly-adsorbed $FeCp_2$ is released below 200 ˚C) occurs under air at 200 °C, indicated by a change of color from yellow to brown attributed to Fe^{2+} oxidation to Fe^{3+}. As shown in Figure 1a, this is followed by the loss of organic Cp rings (18 wt.%) at 300 ˚C, which matches with the theoretical weight loss for the organic attributed to encapsulated remaining ferrocene (25.6 wt.% $FeCp_2$ with 70 wt.% organic).

The release of the organic ligand from MOF (1,4-benzedicarboxylate, BDC) occurs between 300-400 °C, which is much lower temperature than for the unaltered (Al)MIL-53 (500-600 °C). Similar low thermal stability under air has been measured for the Fe-containing isoreticular MOF ((Fe)MIL-53)[7]. This suggests chemical interaction between ferrocene-derived Fe oxides species with [AlO_6] mono-dimensional structural building unit (SBU), weakening the pristine carboxylate-aluminum bonds leading to lower thermal stability. This may be caused by a homogeneous integration of Fe sites atomically dispersed along the crystalline scaffold, as a similar effect has been previously demonstrated in other MOFs by trans-metalation[7] or incorporation of metal atom or clusters via atomic layer deposition[8].

According to the oxidized ferrocene remaining within MOF pores, Fe-Al oxide inorganic residue (32.5 wt.%) must contain 7.7 wt.% of Fe upon full organic calcination at 500 °C, and 24.8 wt.% Al_2O_3 species resulting from (Al)MIL-53 framework. This matches with the theoretically 23.8 wt.% of Al_2O_3 calculated by BDC/Al_2O_3 ratio from TGA analysis of pure MOF under air. This results in a bimetallic Fe-Al oxide containing approximately **1 Fe : 3 Al,** as confirmed by ICP (see Table S1).

In-situ XRD analysis in Figure 1b (see also Figure S2-S3) shows the evolution of the crystalline structure of $FeCp_2$@MOF at increasing temperature under air. The gas-phase infiltration of $FeCp_2$ on the evacuated MOF results in the transformation of the large-pore (LP) into closed-pore (CP) crystalline phase[9]. Surprisingly, the material recovers its large-pore (LP) phase upon oxidation of infiltrated $FeCp_2$ at 200 °C, although the organic component (Cp) may be still occupying the MOF pores as oxidized ferrocene according to TGA in air and the remaining surface area, as discussed later. No apparent change on the crystalline structure happens upon evacuation of the organic Cp components at 300 °C, which confirms the preservation of the integrity of MOF crystalline framework during the oxidation-decomposition of ferrocene. Curiously, MOF containing FeO_x species does not show the same reversible pore structure as commonly observed for empty MOF upon exposure to atmospheric moisture[10], suggesting the occupancy of pores by the FeO_x species impeding the pores closure. No apparent diffraction peaks are observed upon calcination of the organic MOF ligand at 500 °C, indicating the amorphous nature of the resulting Fe-Al oxide species. Very small nanocrystalline domains (below 1 nm) may be formed, usually associated to very broad diffraction peaks. A clear formation of larger crystalline phases, such as iron oxide, aluminum oxide and iron-aluminum oxide spinel, are identified at 1000 °C (see Figure S4), which may be attributed to the segregation/sintering of the initial amorphous/small Fe-Al oxide species present from 500 °C up to 1000 °C into more stable phases. For instance, transient $FeAl_2O_4$ crystalline phase species visible at 1000 °C, but starts segregating into both iron and aluminum oxides after 30 min at 1000 °C.

As shown by N_2 sorption isotherms in Figure 2c, complete evaporation at 300 °C of cyclopentadienyl-derived organic species occupying the MOF cavities results in a significant liberation of surface area (856 m^2/g) compared to the unaltered non-porous $FeCp_2$@(Al)MIL-53 (because of the high loading of organometallic[6]). The presence of FeO_x species decorating the interior of (Al)MIL-53 channels is supported by a significant decrease in surface area compared to empty MOF (1608 m^2/g) and also empty MOF treated at 300 °C under air (1342 m^2/g). As shown in pore distribution plot in Figure 1d, the presence of FeO_x within MOF pores at 300 ˚C resulted in a sharpening down of the pore distribution peak centered at 1 nm compared to the empty MOF treated at 300 °C. Micropores around 1 nm at 300 °C are converted into *ca* 50 nm mesopores at 500 °C, due to the complete elimination of the organic ligand (BDC) and consequent collapse of the channels into mesoporous snowflake-like nanostructures. This exotic nanostructure is directed by the templating-effect of the AlO_6 monodimensional SBUs of the unaltered crystalline MOF structure, which also facilitates that FeO_x species on MOF at 300 ˚C preserve their dispersion upon the structural collapse at 500 ˚C. It is noteworthy to mention that the presence of FeO_x species contribute to the resulting nanostructure, as seen when contrasting surface area and mesoporosity against the bare MOF treated at 500°C.

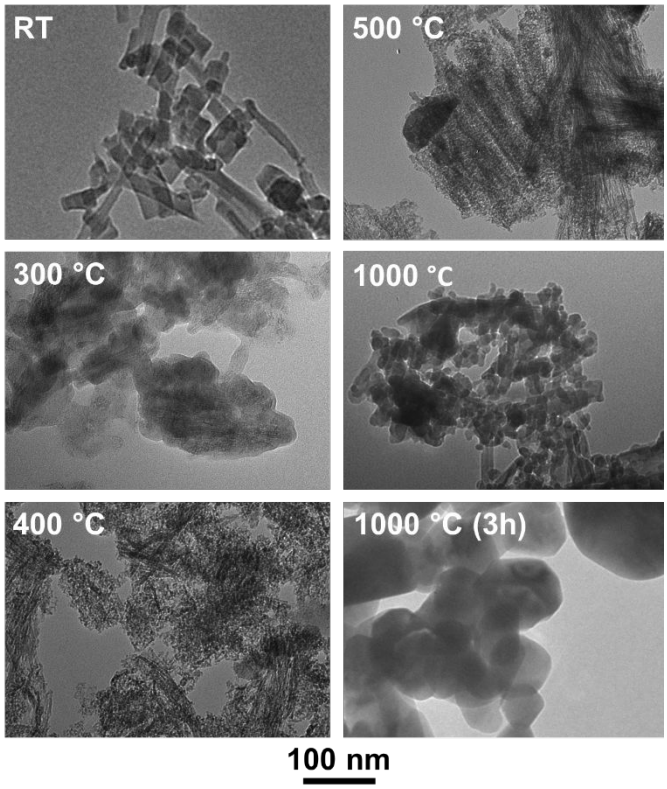

Figure 2. TEM analysis of $FeCp_2$@MOF treated at different temperatures under air.

FTIR analysis supports the evolution between large-pore (LP) into closed-pore (CP) due to ferrocene inclusion, as observed by XRD, which is identified by shifts on the IR bands attributed to asymmetric and symmetric carboxylate stretching[6] at 1400-1600 cm^{-1}. In addition, IR bands associated with organic components disappear at 500 ˚C due to the complete calcination of the organic framework. Interaction between ferrocene and free hydroxyl located at the MOF channels is indicated by the OH vibrational band at 3600 cm^{-1}, which is attenuated, broadened, and shifted for ferrocene-loaded material compared to bare MOF (see Figure S5). The presence of free hydroxy groups pointing at the center of MOF nanochannels[11] may be promoting the decomposition of the $Fe(II)Cp_2$ into Fe (III) oxide species under air at 200 °C, as previously reported for the decomposition of ferrocene into oxidized iron species under the presence of oxalic acid at 177 °C[12]. Furthermore, hydroxy groups may stabilize single iron oxide species, as recently observed for $Fe(OH)_3$ species formed by decomposition of ferrocene over Pt under similar aerobic conditions[13]. DRIFT analysis of $FeCp_2$@MOF treated at 300 °C reveals the recovery of the pristine OH groups at 3700 cm^{-1} (upon water evacuation at 200 °C), as observed for MOF evacuated under the same conditions (see Figure S6).

TEM analysis of the microstructure of $FeCp_2$@MIL-53 upon treatment with air at different temperatures is shown in Figure 2. Pristine MOF nanorod morphology combines into larger aggregates but exhibits 1-nm mono-dimensional channels at 300 °C, which supports the preservation of the MOF order and porosity as discussed above. Similar morphology is observed for empty MOF treated at 300 °C (see Figure S7). Between 300-500 °C, organic ligands are completely released according to TGA. This results in the formation of nanostructured bimetallic oxides which exhibit needle-like shapes intercalated with more rounded species, forming a shape reminiscent of a snowflake. A progressive melting of this nanostructure into larger particles is observed at temperatures above 700 °C (see Figure S8), eventually leading to the formation of non-porous particles at 1000 °C and longer hold times. HR-TEM analysis of $FeCp_2$@MOF_{500C} (see Figure S9) provided better resolution of the fibrous and porous structure of the resulting materials ruling out the presence of large iron oxide crystalline particles, which supports the theory of homogeneous Fe-Al oxide phases. HDAAF-STEM-EDS analysis for $FeCp_2$@MOF treated at 280 ˚C and 400 ˚C also confirmed that the presence of Fe and Al is very homogenous along the catalysts (See Figure S10-S11). The novel catalyst contains a high concentration of well-dispersed Fe (17.3 wt.%Fe), well-dispersed on aluminum oxide(25.9 wt.% Al), which exhibits elevated active metal surface area (33 $\mu mol_{CO}/g$), as determined by CO chemisorption (See Table S2). This can have very interesting catalytic properties for several applications.

A possible mechanism of metallocene@MOF transformation into mixed metal oxide under air is illustrated in Scheme 1. At 200 °C, only oxidized ferrocene remains within the MOF pores while weakly adsorbed ferrocene is evaporated. Organic species resulting from the oxidation of the ferrocene are completely evacuated at 300 °C, leading iron oxide cluster-like species dispersed along the MOF channel liberating considerable surface area (856 m^2/g). Between 300-400 °C, the organic ligand bridging the MOF framework is oxidized to CO_2, which leads to the collapse of the structure into a snow-flake morphology containing Fe-Al oxide species and hierarchical micro/mesoporous structure (289 m^2/g). The nanostructured amorphous bimetallic oxide morphology melts into non-porous large particles (above 20 nm) exhibiting phase segregation at high temperatures (1000 °C).

In order to evaluate the generality of the approach, we have evaluated the gas-phase infiltration of other commercially

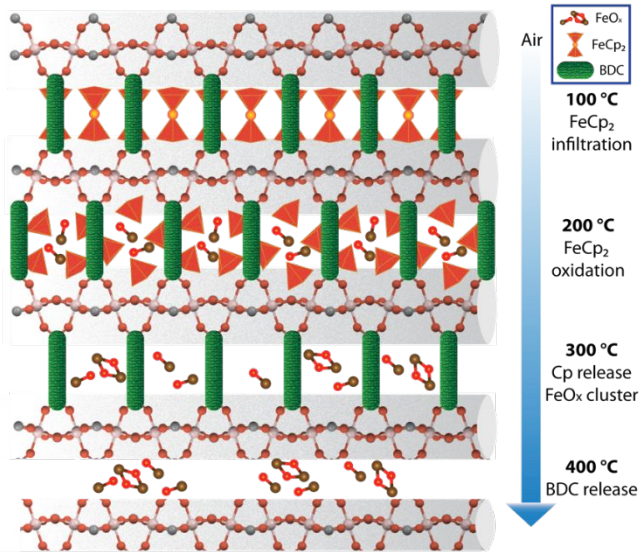

Scheme 1. Illustrative description of $FeCp_2$@MOF structural evolution at increasing temperatures under air.

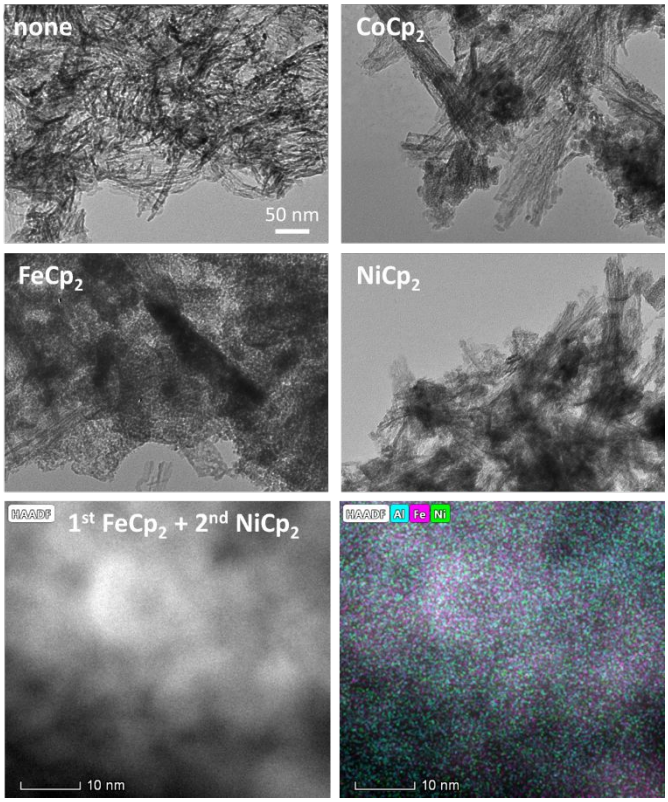

Figure 3. (above) TEM images for different metallocene@MOF calcined at 500 ˚C compared to bare MOF to illustrate generality of the approach. (below) STEM-HAADF and EDS mapping for second loading with $NiCp_2$ on $FeCp_2$@MOF_{300C}, and subsequent treatment at 500 ˚C.

available volatile metallocenes on (Al)MIL-53, such as $CoCp_2$ and $NiCp_2$, and also $NiCp_2$ on (Fe)MIL-53, which resulted in very similar results compared to $FeCp_2$@(Al)MIL-53. Moreover, we also evaluated the incorporation of $FeCp_2$ in isoreticular (Fe)MIL-53. In all the cases, characterization data reveals similar results as measured for $FeCp_2$@(Al)MIL-53 (Figure S12-S17 and Table S1). As illustrated in Figure 3, TEM images for Fe, Co, and Ni metallocene infiltrated on (Al)MIL-53 show the same morphology as $FeCp_2$@(Al)MIL-53 upon calcination at 500 °C under air. Furthermore, we also demonstrated that the remaining porosity of $FeCp_2$@(Al)MIL-53 material treated at 300 °C can be gas-phase reloaded with a different metallocene (i.e. $NiCp_2$) preserving the snowflake morphology as well as the excellent dispersion and homogeneity upon final treatment at 500 ˚C, as confirmed by STEM analysis (see Figure 3 and S18-S19). This demonstrates the potential of this general synthetic route to prepare multi-metal oxide materials with more than two metals for several applications, including both catalysis and electrocatalysis[14].

Fe-Al oxide material derived from $FeCp_2$@(Al)MIL-53 treated at 500 ˚C was tested as catalysts for ammonia synthesis at low temperatures under the conditions reported in our previous work with Ru catalysts derived from (Ru)HKUST-1[1]. MOF-derived Fe catalysts exhibit a Fe loading of 17.3 wt.% and dispersion of 2%, according to the results obtained by ICP and CO chemisorption, respectively (see Table S2 and Figure S20). This is translated to almost one order of magnitude higher catalytic activity per gram of Fe for ammonia synthesis at lower temperatures (<400 ˚C) compared to commercial Fe catalysts exhibiting very low Fe dispersion. Further development and optimization of these MOF-derived iron catalysts can lead to catalysts exhibiting higher Fe dispersion at high Fe loading, in contrast to current methodologies showing an inversely proportional relationship between dispersion and loading: i.e. high dispersion at low loading (FeO_x/γ-Al_2O_3)[15] or low dispersion at high loading (current commercial catalyst). In addition, the calcination under air at 500 °C of the $FeCp_2$@(Al)MIL-53 precursor resulted in highly porous (*ca* 300 m^2/g) amorphous material combining micro and mesoporosity, which exhibits higher porosity than an iron oxide catalysts supported on commercial γ-Al_2O_3 via conventional impregnation (Figure S21). This is translated into enhanced ammonia rates at low temperatures compared to the state of the art.

We reported a general technique consisting in the use of volatile metallocenes infiltrated within MOF pores in a guest@host configuration as catalyst precursor for multi-metal oxide materials via calcination under air. This approach provides a versatile synthesis strategy to disperse and stabilize catalytically active metal species on porous metal oxide supports to design advanced catalysts and electrocatalyst for several applications of industrial interest, such as energy storage and ammonia synthesis.

References

1. I. Luz, et al., *Catal. Sci. Technol.*, 2020, **10**, 105-112.
2. I. Agirrezabal-Telleria, et al., *Nat. Commun.*, 2019, **10**, 2076; L. Oar-Arteta, et al., *Materials Chemistry Frontiers*, 2017, **1**, 1709-1745; N. Saadatjou, A. Jafari and S. Sahebdelfar, *Chem. Eng. Commun.*, 2015, **202**, 420-448.
3. I. Luz, M. Soukri and M. Lail, *Chem. Commun.*, 2018, **54**, 8462-8465; K. J. Lee, J. H. Lee, S. Jeoung and H. R. Moon, *Acc. Chem. Res.*, 2017, DOI: 10.1021/acs.accounts.7b00259.
4. D. Esken, et al., *Chem. Mater.*, 2010, **22**, 6393-6401; M. Mueller, et al., *Chem. Mater.*, 2008, **20**, 4576-4587; M. Mueller, O. I. Lebedev and R. A. Fischer, *J. Mater. Chem.*, 2008, **18**, 5274-5281; F. Schröder, S. Henke, X. Zhang and R. A. Fischer, *Eur. J. Inorg. Chem.*, 2009, **2009**, 3131-3140; M. Meilikhov, et al., *Eur. J. Inorg. Chem.*, 2010, DOI: 10.1002/ejic.201000473, 3701-3714.
5. I. Luz, et al., *Eur. J. Inorg. Chem.*, 2015, **2015**, 3904-3912.
6. M. Meilikhov, K. Yusenko and R. A. Fischer, *Dalton Trans.*, 2009, DOI: 10.1039/B820882B, 600-602.
7. D. Y. Osadchii, et al., *ACS Catal.*, 2018, **8**, 5542-5548.
8. T. Ikuno, et al., *J. Am. Chem. Soc.*, 2017, **139**, 10294-10301.
9. M. Meilikhov, K. Yusenko and R. A. Fischer, *Dalton Trans.*, 2010, **39**, 10990-10999.
10. A. Boutin, et al., *Microporous Mesoporous Mater.*, 2011, **140**, 108-113.
11. M. Meilikhov, K. Yusenko and R. A. Fischer, *J. Am. Chem. Soc.*, 2009, **131**, 9644-9645.
12. A. Bhattacharjee, et al., *J. Mater. Sci.*, 2013, **48**, 2961-2968.
13. L. Cao, et al., *Nature*, 2019, **565**, 631-635.
14. S. Yang, L. Peng, S. Bulut and W. L. Queen, *Chemistry – A European Journal*, 2019, **25**, 2161-2178.
15. S. Mosallanejad, B. Z. Dlugogorski, E. M. Kennedy and M. Stockenhuber, *ACS Omega*, 2018, **3**, 5362-5374; F. Ding, et al., *Ind. Eng. Chem. Res.*, 2014, **53**, 17563-17569; J.-Y. Park, et al., *J. Mol. Catal. A: Chem.*, 2010, **323**, 84-90.

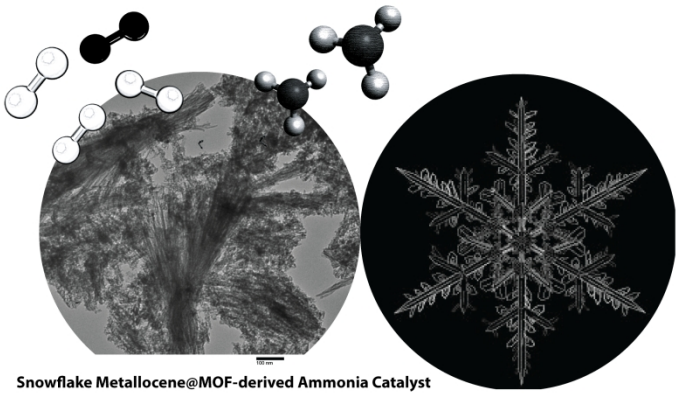

Metallocene infiltrated on porous metal organic frameworks can be tailored as versatile precursors to design nanostructured multi-metal oxide catalysts for emerging applications such as ammonia synthesis at lower temperature.